

Electron-hole superfluidity controlled by a periodic potential

Oleg L. Berman^{1,2}, Roman Ya. Kezerashvili^{1,2}, Yurii E. Lozovik^{3,4}, and Klaus G. Ziegler⁵

¹*Physics Department, New York City College of Technology, The City University of New York, Brooklyn, NY 11201, USA*

²*The Graduate School and University Center, The City University of New York, New York, NY 10016, USA*

³*Institute of Spectroscopy, Russian Academy of Sciences, 142190 Troitsk, Moscow, Russia*

⁴*Research University Higher School of Economics, Moscow, Russia 101000*

⁵*Institut für Physik, Universität Augsburg D-86135 Augsburg, Germany*

(Dated: June 25, 2019)

We propose to control of an electron-hole superfluid in semiconductor coupled quantum wells and double layers of two-dimensional (2D) material by an external periodic field. This can either be created by the gates periodically located and attached to the quantum wells or double layers of 2D material or by the Moiré pattern of two twisted layers. The dependence of the electron-hole pairing order parameter on the temperature, the charge carrier density, and the gate parameters is obtained by minimization of the mean-field free energy. The second order phase transition between superfluid and electron-hole plasma, controlled by the external periodic gate field, is analyzed for different parameters.

I. INTRODUCTION

The system of spatially separated electrons and holes can be realized in semiconductor coupled quantum wells (CQWs), where electrons and holes are located in different quantum wells. For low temperatures and weak attraction the Bardeen-Cooper-Schrieffer (BCS) approach describes the superfluid formed by coherent Cooper pairs, while in the strong attraction regime the composite bosons, known as indirect (dipolar) excitons, are formed. An electron-hole plasma (EHP) appears at sufficiently higher temperatures. Superfluidity in the two-dimensional (2D) system with spatially separated electrons and holes was predicted using the BCS mean-field approach [1], which caused intensive theoretical [2–11] as well as experimental studies [12–22]. Different electron-hole phases, characterized by unique collective properties, have been analyzed in the system of spatially separated electrons and holes [23]. The BCS phase of electron-hole Cooper pairs in a dense electron-hole system [1] and a dilute gas of indirect excitons, formed as bound states of electron-hole pairs, were also analyzed in CQWs [24]. Superfluidity of the BCS phase, formed by spatially separated electrons and holes, can be manifested as non-dissipative electric currents and quasi-Josephson phenomena [1, 2]. Besides the superfluid phase a Wigner supersolid state caused by dipolar repulsion in electron-hole double layers was described [25–28]. The recent theoretical and experimental achievements in the studies of the superfluid dipolar exciton phases in CQWs were reviewed in Ref. [29]. Probing the ground state of an electron-hole double layer by low temperature transport was experimentally performed [30], and the various experimental studies of excitonic phases in CQWs were described in Ref. [31].

Another physical realization for indirect excitons, formed in an electron-hole double layer, is a wide single GaAs/AlGaAs quantum well with a finite width [32]. In a wide single QW, the transverse electric field separates electrons and holes at the different boundaries of the QW [32]. The advantage of a wide single QW compared with CQWs is the smaller number of the QW boundaries, which leads to the increase of the electron mobility. Based on the photoluminescence pattern caused by electron-hole recombination, the evidence for a condensate of indirect excitons, electrically polarized in a GaAs wide single QW, was achieved experimentally recently for the thickness of 15 nm of the quantum well at the temperature $T = 370$ mK [33]. A spontaneous condensation of trapped two-dimensional dipolar excitons from an interacting gas into a dense liquid state was observed in GaAs/AlGaAs CQWs with an interwell separation $D = 4$ nm at the temperatures below a critical temperature $T_c \approx 4.8$ K [34]. The transport of indirect excitons with an interwell separation $D = 4$ nm in GaAs/AlGaAs CQWs in linear lattices, created by laterally modulated gate voltage with a lattice period $b = 2 \mu\text{m}$, was studied experimentally at the temperatures $T = 1.6$ K and $T = 6$ K, and the localization-delocalization transition for transport across the lattice was observed with reducing lattice amplitude or increasing exciton density [35].

Besides semiconductor CQWs, the superfluid system of spatially separated electrons and holes can ap-

pear in a graphene double layer [11, 36–39], two opposite surfaces of the film of topological insulators [40], two layers with composite fermions in the quantum Hall regime at the filling factor $\nu = 1/2$ [41].

Today an intriguing counterpart to gapless graphene is a class of monolayer direct bandgap materials, namely transition metal dichalcogenides (TMDCs). Monolayers of TMDC such as MoS_2 , MoSe_2 , MoTe_2 , WS_2 , WSe_2 , and WTe_2 are 2D semiconductors, which have a variety of applications in electronics and opto-electronics [42]. The strong interest in TMDC monolayers is motivated by the following facts: a semiconductor band structure is characterized by a direct gap in the single particle spectrum [43], the existence of excitonic valley physics, and the possibility of an electrically tunable, strong light-matter interactions [44, 45]. Monolayers of transition metal dichalcogenides are truly 2D semiconductors, which hold great appeal for electronics and opto-electronics applications due to their direct band gap properties. Monolayer TMDCs have already been implemented in field-effect transistors, logical devices, and lateral and tunneling optoelectronic structures [42]. Like graphene, the monolayer TMDCs have hexagonal lattice structures, and the extrema (valleys) in the dispersion relations of both the valence and conduction bands can be found at the \mathbf{K} and $-\mathbf{K}$ points of the hexagonal Brillouin zone. However, unlike graphene, these 2D crystals do not have inversion symmetry [42].

High-temperature superfluidity can be studied in a heterostructure of two TMDC monolayers, separated by a hexagonal boron nitride (*h*-BN) insulating barrier [46]. The dipolar excitons were observed in heterostructures formed by monolayers of MoS_2 on a substrate constrained by hexagonal boron nitride layers [47]. The theoretical study of the phase diagram of 2D condensates of indirect excitons in a TMDC double layer was reported [48]. The high-temperature superfluidity of the two component Bose gas of A and B dipolar excitons in a transition metal dichalcogenide double layer was predicted in Refs. [49, 50].

In this paper we study how the BCS-like EHP-superfluid phase transition can be controlled by the external periodic field, applied to the spatially separated electrons and holes via the gates periodically attached to CQWs, where a quasi-two-dimensional system of charge carriers is formed. The external periodic field, applied to the spatially separated electrons and holes can be also produced via the gates periodically attached to double layers of 2D material or a twisted TMDC double layer, where a truly 2D system of charge carriers is formed. For this purpose we employ a mean-field approximation for the many-body system of electrons and holes, using the partition function of the grand-canonical ensemble at the temperature T and the chemical potentials of the electrons and the holes, respectively. The latter represent the Fermi energies of the electrons and the holes. The logarithm of the partition function gives us immediately the free energy, whose minimum defines the mean-field solution with a non-vanishing order parameter of the superfluid phase. We also briefly discuss quantum fluctuations around the mean-field solution and how to measure them in terms of the static structure factor. The main goal, though, is to analyze the influence of the external periodic field on the critical temperature of the EHP-superfluid transition in an electron-hole double layer.

The paper is organized in the following way. We obtain the free energy of the electron-hole double layer in the external periodic potential and study the second order EHP-superfluid transition using a Landau expansion of the free energy in Sec. II. The results of calculations are presented and analyzed in Sec. III. Finally, the discussion of the results and the conclusions follow in Sec. IV.

II. PHASE TRANSITION IN THE ELECTRON-HOLE DOUBLE LAYER UNDER THE ACTION OF THE EXTERNAL PERIODIC POTENTIAL

The Hamiltonian of the system of spatially separated electrons and holes in momentum representation can be written as

$$H = \sum_{\mathbf{p}} \sum_{\sigma=e,h} \varepsilon_{\mathbf{p},\sigma} c_{\mathbf{p}\sigma}^\dagger c_{\mathbf{p}\sigma} + \sum_{\mathbf{p}, \mathbf{p}_1, \mathbf{p}_2} U_{\mathbf{p}} c_{\mathbf{p}-\mathbf{p}_1, h}^\dagger c_{\mathbf{p}-\mathbf{p}_2, h} c_{\mathbf{p}_1, e}^\dagger c_{\mathbf{p}_2, e}, \quad (1)$$

where $c_{\mathbf{p},e}^\dagger$ ($c_{\mathbf{p},e}$) is the creation (annihilation) operator for electrons, and $c_{\mathbf{p},h}^\dagger$ ($c_{\mathbf{p},h}$) is the corresponding operator for holes. The electron and hole single-particle energy spectra $\varepsilon_{\mathbf{p},\sigma}$ are defined below in the tight-binding approximation, reflecting the external periodic field applied to the CQWs or double layers of 2D material. The electron-hole attraction potential in momentum space $U_{\mathbf{p}}$ is defined below. In Eq. (1) the spins of electrons and holes are neglected, because we are not interested in magnetization effects.

We consider an external periodic potential induced by the gate $V(\mathbf{r})$ forming either a 1D or a 2D square superlattice with the period b applied to the electron and hole quantum wells. As an example,

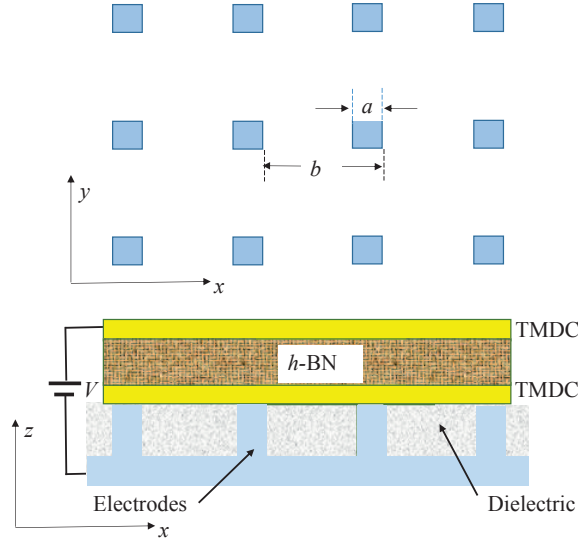


FIG. 1: Schematic electrode pattern in the $x - y$ and $z - x$ planes.

the particular case related to the phase transition of indirect excitons in a double layer, formed by two TMDC monolayers that are separated by h -BN, since h -BN monolayers are characterized by relatively small density of the defects of their crystal structure monolayers. In Fig. 1 a schematic electrode pattern in the $x - y$ and $z - x$ planes is presented. In our calculations we consider the TMDC monolayers to be separated by h -BN insulating layers and the separation between two layers of TMDC materials calculated in steps of $D_{hBN} = 0.333$ nm, corresponding to the thickness of one h -BN monolayer [46]. Therefore, the interlayer separation D is presented as $D = N_L D_{hBN}$, where N_L is the number of h -BN monolayers, placed between two TMDC monolayers. It is obvious that the strength of the electron-hole interaction decreases with the increase of the separation between the layers. We assume that the densities of electrons and holes are equal in order to have a neutral electron-hole plasma and because the electrons and holes are created always pairwise by an external laser source. This implies that the corresponding chemical potentials are also equal. Periodically positioned gates under the same electric potentials create in a turn the periodical potential in the 2D system under consideration.

When the electron-hole attraction leads to Cooper pairing of electrons and holes, characterized by the order parameter Δ [51, 52], the free energy is described within the mean-field approximation (MFA) [1, 53]. Following Ref. [53], and assuming that (i) the order parameter Δ does not depend on the momentum, and (ii) the dispersion relation $\varepsilon_{\mathbf{p},e} = \varepsilon_{\mathbf{p},h} = \varepsilon_{\mathbf{p}}$ is the same for electrons and holes, the MFA of the free energy at temperature T ($\beta = 1/k_B T$, where k_B is the Boltzmann constant) as a function of the dimensionless order parameter $\gamma = \beta|\Delta|$ can be written as

$$F = -\frac{1}{\beta^2 u_0} \gamma^2 - \frac{1}{|B|\beta} \int_B \ln \left[2 \left(1 + \cosh \left(\sqrt{\beta^2 \varepsilon_{\mathbf{p}}^2 + \gamma^2} \right) \right) \right] d^2 p. \quad (2)$$

In Eq. (2) the integration over the momentum \mathbf{p} is taken over the Brillouin zone with area $|B|$ and u_0 is the strength of the electron-hole interaction given by

$$\frac{1}{u_0} = \frac{1}{|B|} \int_B \frac{1}{U_{\mathbf{p}}} d^2 p < 0, \quad (3)$$

which parametrically depends on the inter layer separation D .

Let us rewrite Eq. (2) in the form of a dimensionless free energy $f = -u_0 F / (k_B T)^2$ and expand the latter in terms of the order parameter γ^2 as $f = f_0 + f_2 \gamma^2 + f_4 \gamma^4$ (Landau expansion [54, 55]). The corresponding coefficients for this expansion are given in Appendix A by Eqs. (A4) - (A6). At the point of the phase transition we have zero order parameter $\gamma = 0$, and the condition for the minimum of the

free energy is $\left. \frac{\partial f}{\partial \gamma^2} \right|_{\gamma=0} = f_2 = 0$. Therefore, the critical point is defined by a vanishing coefficient f_2 . Thus from expression (A5) follows that the critical inverse temperature β_c satisfies the condition

$$\frac{1}{u_0} = -\frac{1}{|B|} \int_B \frac{\tanh(\beta_c |\epsilon_{\mathbf{p}}|)}{|\epsilon_{\mathbf{p}}|} d^2 p = - \int_{E_0}^{E_1} \frac{\tanh(\beta_c |2tE - \delta_0|)}{|2tE - \delta_0|} \rho(E) dE. \quad (4)$$

Here we have used the fact that the p integration can be expressed as an energy integration through the relation $d^2 p/|B| = \rho(E)dE$, where $\rho(E)$ is the density of states of the non-interacting Hamiltonian with dispersion $\epsilon_{\mathbf{p}}$. The dimensionless energy parameter $E = (\delta_0 - \epsilon_{\mathbf{p}})/2t$ is derived from the dispersion which is shifted by the Fermi energy δ_0 . The integration is restricted to the interval $[E_0, E_1]$, since only electronic states are accessible within the main band of the electronic band structure. The specific values depend on the material and its dispersion, typically for a parabolic dispersion they are given by $E_0 \approx 0$ and $E_1 \approx \hbar^2/(\lambda^2 2m)$ with the lattice constant λ of the underlying material.

The relation between u_0 and β_c in Eq. (4) indicates that an increasing interaction strength $-u_0$ implies an increasing critical temperature. Moreover, $\tanh(\beta_c |2tE - \delta_0|)/|2tE - \delta_0|$ is a monotonically decreasing function of $|2tE - \delta_0|$ with the maximum at $E = \delta_0/2t$. The density of states $\rho(E)$, on the other hand, distinguishes between the case of a parabolic dispersion ($\rho(E) = \text{const.}$) and the case of a periodic potential, where $\rho(E)$ is not constant. Thus the goal is to design the dispersion by adding a superstructure to the material. This can either be achieved by doping [56], by creating a gated periodic potential on the 2D material [35] (cf. Fig. 1) or by twisting the two layers relative to each other to create a Moiré pattern [57, 58]. Then the density of states can be chosen such that it picks up the maximum value of the integrand $\tanh(\beta_c |2tE - \delta_0|)/|2tE - \delta_0|$. Although this depends on the Fermi energy δ_0 , the latter can also be tuned by a uniform external gate to obtain a large value for the integral. As an example we consider the tight-binding approximation on a square lattice with periodicity b . Then the electron and the hole dispersion reads [59–61]:

$$\epsilon_{\mathbf{p}} = \delta_0 - 2t \cos(p_x b/\hbar) - 2t \cos(p_y b/\hbar) \quad (-\pi \leq p_{x,y} b/\hbar < \pi), \quad (5)$$

which has a band width $8t$. The corresponding density of states reads [62]

$$\rho(E) = \rho_0 \frac{K\left(\frac{2-|E|}{2+|E|}\right)}{2+|E|} \quad (-2 \leq E \leq 2), \quad (6)$$

where $K(x)$ is the complete elliptic integral of the first kind and ρ_0 is a normalization factor. In Appendix B are given the expressions for the coefficients f_0 , f_2 and f_4 of the Landau expansion in the case of the periodical potential. For the dispersion (5) we have derived some results directly from Eqs. (2) and (4), which will be discussed in the next section.

Instead of the 2D periodic potential we could also consider an anisotropic potential with a 1D periodicity, which would also affect strongly the density of states. This case corresponds to the system studied in Ref. [35].

III. RESULTS

The free energy F of Eq. (2) with the dispersion in Eq. (5) is calculated as a function of the dimensionless order parameter γ . The dependence of the dimensionless free energy $f = -\beta^2 u_0 F$ on $t\beta$ and the order parameter γ is shown in Fig. 2. This result demonstrates that f has a minimum with respect to the order parameter γ , while the dependence of f on $t\beta$ is not strong. The non-zero minimum of f with respect to the order parameter γ corresponds to the equilibrium value of γ , characterizing the electron-hole superfluid. The plot in Fig. 2a represents the low-temperature BCS-like superfluid for electron-hole pairing with a non-zero value of the order parameter $\gamma > 0$ at the minimum, while Fig. 2b shows the high-temperature non-superfluid EHP for the zero value of γ at the minimum. Both cases are connected via the second-order phase transition, as visualized in Fig. 3, where the normalized free energy f as a function of the order parameter γ is plotted for different values of βu_0 at fixed parameters $t\beta$ and $\delta_0/2t$. The curves for $\beta u_0 = -50$ and $\beta u_0 = -60$ demonstrate the existence of low-temperature BCS-like superfluid with electron-hole pairing with a non-zero equilibrium value of the order parameter $\gamma > 0$.

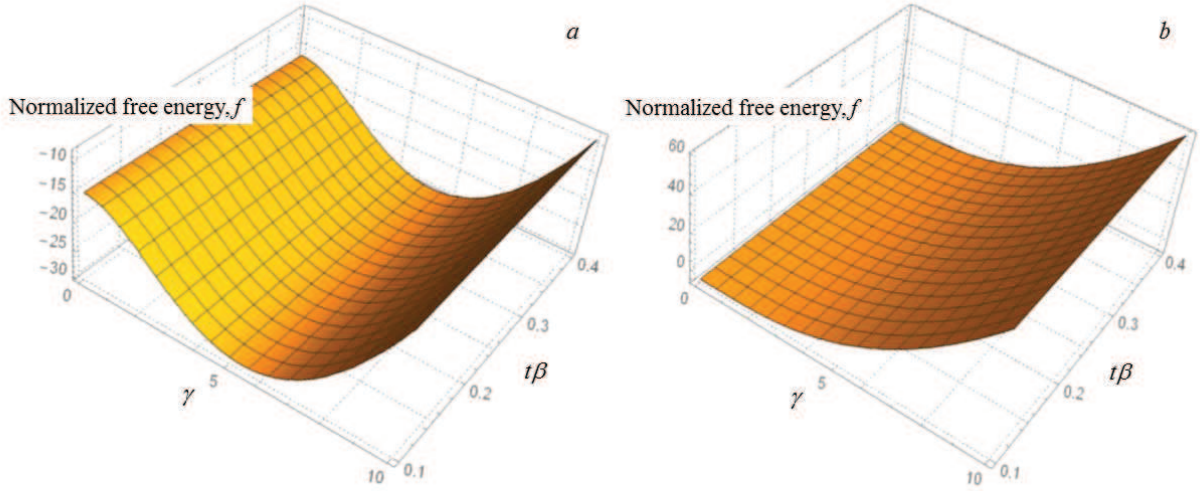


FIG. 2: The normalized free energy f as a function of $t\beta$ and the order parameter γ . (a) $\delta_0/2t = 0.15$; $\beta u_0 = -80$. (b) $\delta_0/2t = 0.15$; $\beta u_0 = -30$.

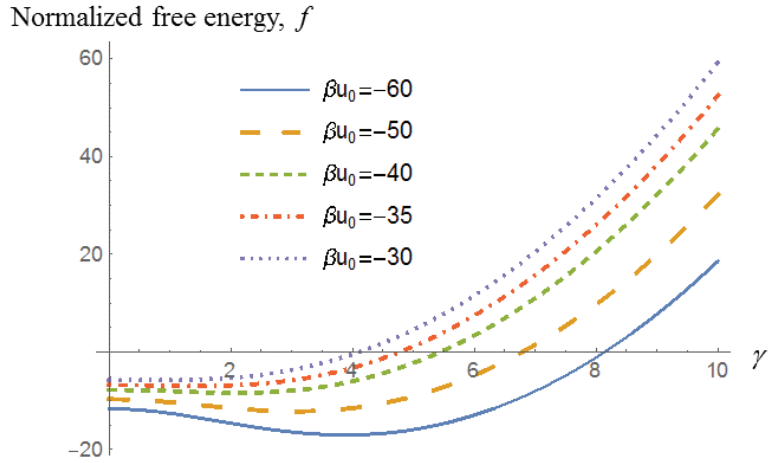


FIG. 3: The normalized free energy f for $\beta u_0 = -30, -35, -40, -50, -60$, at $\beta t = 0.22$ and $\delta_0/2t = 0.175$ indicates a second order phase transition between $\beta u_0 = -50$ and $\beta u_0 = -40$.

The second order phase transition is characterized by the equilibrium value $\gamma = 0$, which corresponds to the values of the parameter βu_0 between $\beta u_0 = -50$ and $\beta u_0 = -40$, as it is shown in Fig. 3. According to Fig. 3, for fixed parameters $\delta_0/2t$ and $t\beta$, the minimal order parameter γ increases with decreasing βu_0 if $\beta u_0 < -50$. The curves in Fig. 3 for $\beta u_0 = -30$ and $\beta u_0 = -35$ represent the high-temperature non-superfluid EHP with $\gamma = 0$.

Fig. 4 can be understood as a $k_B T - u_0$ phase diagram, in which the different curves indicate the phase boundaries between the EHP on the left and the superfluid on the right for different values of the

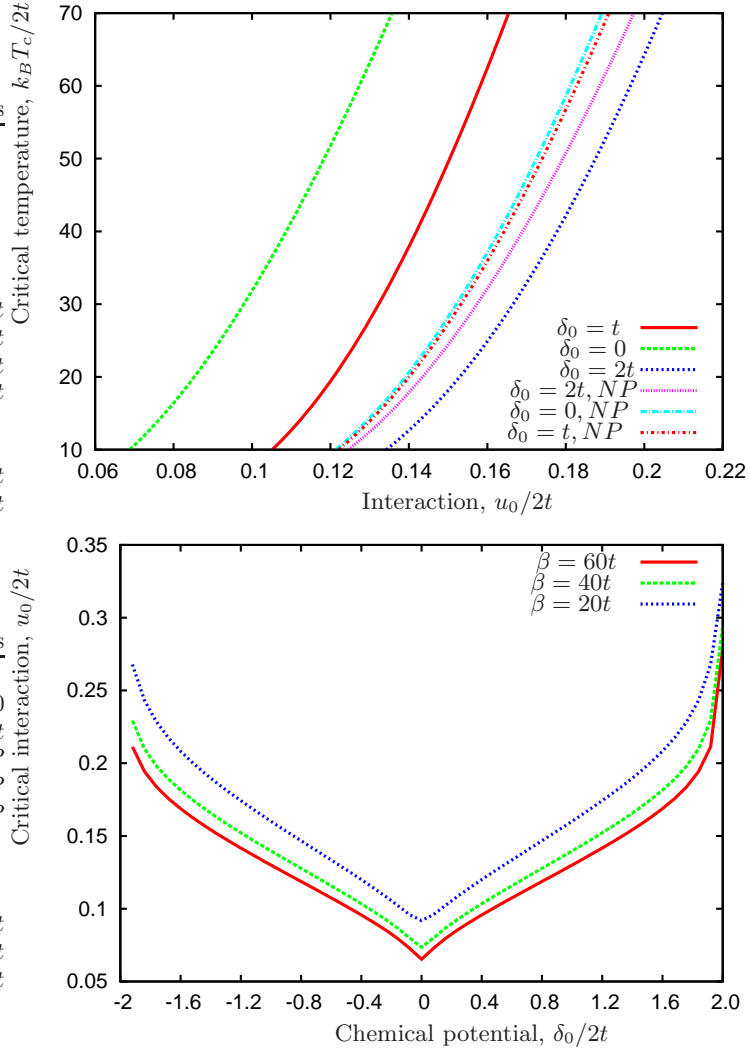


FIG. 4: a) Critical temperature as a function of the interaction parameter for different normalized Fermi energies $\delta_0/2t$. The curves with index *NP* are without periodic potential, while the other curves are for a periodic potential in tight-binding approximation of Eq. (5).

b) Critical interaction strength at three fixed inverse temperatures β as a function of the Fermi energy $\delta_0/2t$.

Fermi energy in the case of a parabolic dispersion ($V = 0$) and the case of a periodic potential with dispersion (5). In the presence of the periodic potential the phase boundaries are more separated for the three values of the Fermi energy $\delta_0 = 0, 0.5t, t$ than those of the parabolic dispersion. On the other hand, all phase boundaries of the latter occur at smaller values $-u_0$ than those of periodic potential if $\delta_0 = t$.

IV. DISCUSSION AND CONCLUSIONS

In the framework of the mean-field approach for electron-hole pairing, we applied the tight-binding approximation for the single electron spectrum of the superlattice created by the external periodic potential and studied the effect of an additional periodic potential on the EHP-superfluid transition. We have assumed for simplicity that the dispersion and the Fermi surfaces of the electrons and the holes are the same, and analyzed the phase transition at finite temperatures. Our results clearly indicate the possibility to control the electron-hole superfluid in CQWs or double layers of 2D material by applying an external periodic potential due to an attached periodic gate. An alternative approach is to create a tun-

able periodic lattices in two twisted layers of 2D materials (“magic angle” bilayers) [63]. The analogous effect occurs in a supersolid, where the crystalline long-range order and non-crystalline long-range order co-exist [64–66]. Contrary to a supersolid, where the crystalline phase is formed due to self-organization, the band structure in the system under consideration are induced by the external periodic potential.

A periodic potential creates many bands which are typically separated by gaps. (Neighboring bands can also touch each other at spectral nodes. This case though, is not considered here.) To reduce the calculation to a single band we have assumed that the order parameter $|\Delta|$ is smaller than the gap between the neighboring band. This allows us to use a single band projection, based on a tight-binding model. The single band has a lower band edge at energy E_0 and an upper band edge at energy E_1 , which are the boundaries of integration for the condition of the critical temperature in Eq. (4). The \mathbf{k} integration is determined by the Coulomb interaction. In BCS theory of Cooper pairs only a small interval around the Fermi energy, whose width is given by the Debye energy $\hbar\omega_D$, contributes to an attractive interaction: $E_0 = E_F - \hbar\omega_D$, $E_1 = E_F + \hbar\omega_D$ [51, 67]. This is different in the excitonic case because the attractive Coulomb interaction exists for all energies inside the band.

The critical temperature depends on the chemical potential δ_0 . Typically it decreases when δ_0 moves away from zero, as depicted in Fig. 4. This is also the case in the absence of the periodic potential which has a constant density of states (cf. Fig. 4a).

A one-dimensional periodic potential has an inverse square root singularity at $E = 0$, which can result in an even stronger enhancement of the critical temperature. In that case we must use the density of states $\rho(E_x)$ for a potential varying in x direction. Then the condition in Eq. (4) becomes

$$\frac{1}{u_0} = -\frac{1}{p_1 - p_0} \int_{p_0}^{p_1} \int_{E_0}^{E_1} \frac{\tanh(\beta_c |2tE_x + p_y^2/2m - \delta_0|)}{|2tE_x + p_y^2/2m - \delta_0|} \rho(E_x) dE_x dp_y. \quad (7)$$

A critical assumption in our model is that electrons and holes have the same dispersion. If they had different dispersions we expect a more complex phase diagram (cf. Ref.[53]). It can even affect the form of the order parameter. In our study we assume that the pumping beam is circularly polarized, and hence the excitons are formed only in one of the valleys: \mathbf{K} or $-\mathbf{K}$ [44, 45]. In this study we address the formation of excitons in one of the valleys. Moreover, we can have two electronic species in TMDC materials due to the existence of two valleys [68].

It should be a particular interest to extend our MFA approach to a more complex one with the valley degrees of freedom and the effective coupling between the two valleys included. Another interesting extension of the MFA of the present work would be the inclusion of quantum fluctuations. This would open a wide avenue for measurements of quantum effects near the EHP-superfluid transition as well as inside the EHP and the superfluid through quantum excitations. A first step in this direction was the calculation of the density-density correlation and the structure factor, which indicates a characteristic increase near the transition [69]. Another possibility is to determine quantum transport properties in the EHP and the superfluid.

Acknowledgments

O.L.B. and R.Ya.K. were supported by US Department of Defense under Grant No. W911NF1810433. Yu.E.L. was supported by the Program of Basic Research of HSE and RFBR grants 17-02-01134 and 18-52-00002. K.G.Z. is grateful for support by a grant from the Julian Schwinger Foundation.

Appendix A: Expansion of free energy with respect to the order parameter in Landau form

From Eq. (2) the dimensionless free energy $f = -u_0 F / (k_B T)^2$ can be written as

$$f = \gamma^2 + u_0 \beta \frac{1}{|B|} \int_B \ln \left[2 \left(1 + \cosh \left(\sqrt{\beta^2 \varepsilon_{\mathbf{p}}^2 + \gamma^2} \right) \right) \right] d^2 p. \quad (A1)$$

One can expand the integrant in Eq. (A1) in terms of the power of γ^2 as

$$\ln \left[2 \left(1 + \cosh \left(\sqrt{\beta^2 \varepsilon_{\mathbf{p}}^2 + \gamma^2} \right) \right) \right] = \ln[2(1 + \cosh[\beta |\varepsilon_{\mathbf{p}}|])] + \frac{\tanh \left(\frac{1}{2} \beta |\varepsilon_{\mathbf{p}}| \right)}{2\beta |\varepsilon_{\mathbf{p}}|} \gamma^2$$

$$+ \frac{\beta^2 \varepsilon_{\mathbf{p}}^2 - \beta |\varepsilon_{\mathbf{p}}| \sinh(\beta |\varepsilon_{\mathbf{p}}|)}{8\beta^4 \varepsilon_{\mathbf{p}}^4 (1 + \cosh[\beta |\varepsilon_{\mathbf{p}}|])} \gamma^4 + \dots \quad (\text{A2})$$

Here to obtain the final expression for the coefficients of the expansion we have used the following identities:

$$\sinh 2u = 2 \sinh u \cosh u, \quad 1 + \cosh 2u = 2 \cosh^2 u. \quad (\text{A3})$$

Substituting (A2) into Eq. (A1) we present the dimensionless free energy in the Landau form [54, 55]

$$f = f_0 + f_2 \gamma^2 + f_4 \gamma^4 + \dots,$$

where

$$f_0 = u_0 \beta \frac{1}{|B|} \int_B \ln[2(1 + \cosh[\beta |\varepsilon_{\mathbf{p}}|])] d^2 p, \quad (\text{A4})$$

$$f_2 = 1 + u_0 \beta \frac{1}{|B|} \int_B \frac{\tanh(\frac{1}{2} \beta |\varepsilon_{\mathbf{p}}|)}{2\beta |\varepsilon_{\mathbf{p}}|} d^2 p, \quad (\text{A5})$$

$$f_4 = u_0 \beta \frac{1}{|B|} \int_B \frac{\beta^2 \varepsilon_{\mathbf{p}}^2 - \beta |\varepsilon_{\mathbf{p}}| \sinh(\beta |\varepsilon_{\mathbf{p}}|)}{8\beta^4 \varepsilon_{\mathbf{p}}^4 (1 + \cosh[\beta |\varepsilon_{\mathbf{p}}|])} d^2 p. \quad (\text{A6})$$

Appendix B: Free energy in the case of the periodic potential

The the case of the periodic potential the integration in (A1) as well as in Eqs. (A4) - (A6) is taken over the Brillouin zone, implying $|B|$ is the area of the Brillouin zone (for the square superlattice of the period b : $|B| = (2\pi\hbar)^2/b^2$, and, therefore, the limits of the integration over p_x and p_y are given by $-\pi\hbar/b$ and $\pi\hbar/b$. Assuming that in (A4) - (A6) the single-particle energy dispersions versus momentum for electrons and holes are the same we can calculate f_0 , f_2 and f_4

$$f_0 = u_0 \beta \int_{-2}^2 \frac{\ln[2(1 + \cosh[\beta |\delta_0 - 2tE|])] K\left(\frac{2-|E|}{2+|E|}\right)}{2 + |E|} dE, \quad (\text{B1})$$

$$f_2 = 1 + u_0 \beta \int_{-2}^2 \frac{\tanh(\frac{1}{2} \beta |\delta_0 - 2tE|) K\left(\frac{2-|E|}{2+|E|}\right)}{2 |\delta_0 - 2tE| \times (2 + |E|)} dE, \quad (\text{B2})$$

$$f_4 = u_0 \beta \int_{-2}^2 \frac{\beta^2 (\delta_0 - 2tE)^2 - \beta |\delta_0 - 2tE| \sinh(\beta |\varepsilon_{\mathbf{p}}|)}{8\beta^4 (\delta_0 - 2tE)^4 (1 + \cosh[\beta |(\delta_0 - 2tE)|])} \frac{K\left(\frac{2-|E|}{2+|E|}\right)}{(2 + |E|)} dE, \quad (\text{B3})$$

where $K(k)$ is the complete elliptic integral of the first kind.

-
- [1] Yu. E. Lozovik and V. I. Yudson, Sov. Phys. JETP Lett. **22**, 26 (1975); Sov. Phys. JETP **44**, 389 (1976).
 - [2] S. I. Shevchenko, Phys. Rev. Lett. **72**, 3242 (1994).
 - [3] Xu. Zhu, P. B. Littlewood, M. S. Hybertsen and T. M. Rice, Phys. Rev. Lett. **74**, 1633 (1995).
 - [4] S. Conti, G. Vignale and A. H. MacDonald, Phys. Rev. B **57**, R6846 (1998).
 - [5] M. A. Olivares-Robles and S. E. Ulloa, Phys. Rev. B **64**, 115302 (2001).
 - [6] D. S. L. Abergel, M. Rodriguez-Vega, E. Rossi, and S. Das Sarma, Phys. Rev. B **88**, 235402 (2013).
 - [7] M. Zarenia, A. Perali, D. Neilson, and F. M. Peeters, Sci. Rep. **4**, 7319 (2014).
 - [8] M. Combescot, R. Combescot and F. Dubin, Rep. Prog. Phys. **80**, 066501 (2017).
 - [9] D. V. Fil and S. I. Shevchenko, Low Temp. Phys. **44**, 867 (2018).
 - [10] Yu. E. Lozovik, Physics-Uspekhi **188**, 1203 (2018).
 - [11] A. Perali, D. Neilson, and A. R. Hamilton, Phys. Rev. Lett. **110**, 146803 (2013).

- [12] T. Fukuzawa, E. E. Mendez and J. M. Hong, Phys. Rev. Lett. **64**, 3066 (1990); J. A. Kash, M. Zachau, E. E. Mendez, J. M. Hong and T. Fukuzawa, Phys. Rev. Lett. **66**, 2247 (1991).
- [13] U. Sivan, P. M. Solomon and H. Shtrikman, Phys. Rev. Lett. **68**, 1196 (1992).
- [14] S. A. Moskalenko and D. W. Snoke, *Bose-Einstein Condensation of Excitons and Biexcitons and Coherent Nonlinear Optics with Excitons* (Cambridge University Press, New York, 2000).
- [15] L. V. Butov, A. Zrenner, G. Abstreiter, G. Bohm and G. Weimann, Phys. Rev. Lett. **73**, 304 (1994); L. V. Butov, C. W. Lai, A. L. Ivanov, A. C. Gossard, and D. S. Chemla, Nature **417**, 47 (2002); L. V. Butov, A. C. Gossard, and D. S. Chemla, Nature **418**, 751 (2002).
- [16] L. V. Butov, J. Phys. Condens. Matter **16**, R1577 (2004).
- [17] A. V. Larionov and V. B. Timofeev, JETP Lett. **73**, 301 (2001); A. V. Gorbunov and V. B. Timofeev, JETP Lett. **84**, 329 (2006).
- [18] V. V. Krivolapchuk, E. S. Moskalenko, and A. L. Zhmodikov, Phys. Rev. B **64**, 045313 (2001).
- [19] D. Snoke, S. Denev, Y. Liu, L. Pfeiffer, and K. West, Nature **418**, 754 (2002).
- [20] D. Snoke, Science **298**, 1368 (2002).
- [21] R. Anankine, M. Beian, S. Dang, M. Alloing, E. Cambril, K. Merghem, C. G. Carbonell, A. Lematre, and F. Dubin, Phys. Rev. Lett. **118**, 127402 (2017).
- [22] J. I. A. Li, T. Taniguchi, K. Watanabe, J. Hone, and C. R. Dean, Nature Physics **13**, 751 (2017).
- [23] Yu. E. Lozovik and O. L. Berman, JETP Lett. **64**, 573 (1996).
- [24] O. L. Berman, Yu. E. Lozovik, D. W. Snoke, and R. D. Coalson, Phys. Rev. B **70**, 235310 (2004).
- [25] Yu. E. Lozovik and O. L. Berman, Physica Scripta **58**, 86 (1998).
- [26] G. E. Astrakharchik, J. Boronat, I. L. Kurbakov, and Yu. E. Lozovik, Phys. Rev. Lett. **98**, 060405 (2007).
- [27] A. E. Golomedov, G. E. Astrakharchik, and Yu. E. Lozovik, Phys. Rev. A **84**, 033615 (2011).
- [28] Y. N. Joglekar, A. V. Balatsky, and S. Das Sarma, Phys. Rev. B **74**, 233302 (2006).
- [29] D. W. Snoke, in *Quantum Gases: Finite Temperature and Non-Equilibrium Dynamics* (Vol. 1, Cold Atoms Series), N. P. Proukakis, S. A. Gardiner, M. J. Davis, and M. H. Szymanska, eds., Imperial College Press, London, 2013.
- [30] K. Das Gupta, A. F. Croxall, J. Waldie, C. A. Nicoll, H. E. Beere, I. Farrer, D. A. Ritchie, and M. Pepper, Advances in Condensed Matter Physics, Volume 2011, Article ID 727958.
- [31] L. V. Butov, J. Phys.: Condens. Matter **19**, 295202 (2007).
- [32] V. V. Solov'ev, I. V. Kukushkin, J. Smet, K. von Klitzing, and W. Dietsche, JETP Letters **83**, 553 (2006).
- [33] M. Alloing, M. Beian, M. Lewenstein, D. Fuster, Y. González, L. González, R. Combescot, M. Combescot, and F. Dubin, Europhys. Lett. **107**, 10012 (2014).
- [34] K. Cohen, Y. Shilo, K. West, L. Pfeiffer, and R. Rapaport, Nano Lett. **16**, 3726 (2016).
- [35] M. Remeika, J. C. Graves, A. T. Hammack, A. D. Meyertholen, M. M. Fogler, L. V. Butov, M. Hanson, and A. C. Gossard, Phys. Rev. Lett. **102**, 186803 (2009).
- [36] O. L. Berman, Yu. E. Lozovik, and G. Gumbs, Phys. Rev. B **77**, 155433 (2008).
- [37] Yu. E. Lozovik and A. A. Sokolik, JETP Lett. **87**, 55 (2008); Phys. Lett. A **374**, 326 (2009).
- [38] R. Bistritzer and A. H. MacDonald, Phys. Rev. Lett. **101**, 256406 (2008).
- [39] O. L. Berman, R. Ya. Kezerashvili, and K. Ziegler, Phys. Rev. B **85**, 035418 (2012).
- [40] D. K. Efimkin, Yu. E. Lozovik, and A. A. Sokolik, Phys. Rev. B **86**, 115436 (2012).
- [41] J. P. Eisenstein and A. H. MacDonald, Nature (London) **432**, 691 (2004).
- [42] A. Kormányos, G. Burkard, M. Gmitra, J. Fabian, V. Zólyomi, N. D. Drummond, and V. Fal'ko, 2D Mater. **2**, 022001 (2015).
- [43] K. F. Mak, C. Lee, J. Hone, J. Shan, and T. F. Heinz, Phys. Rev. Lett. **105**, 136805 (2010).
- [44] D. Xiao, G. B. Liu, W. Feng, X. Xu, and W. Yao, Phys. Rev. Lett. **108**, 196802 (2012).
- [45] K. F. Mak, K. He, C. Lee, G. H. Lee, J. Hone, T. F. Heinz, and J. Shan, Nat. Mater. **12**, 207 (2013).
- [46] M. M. Fogler, L. V. Butov, and K. S. Novoselov, Nature Commun. **5**, 4555 (2014).
- [47] E. V. Calman, C. J. Dorow, M. M. Fogler, L. V. Butov, S. Hu, A. Mishchenko, and A. K. Geim, Appl. Phys. Lett. **108**, 101901 (2016).
- [48] F.-C. Wu, F. Xue, and A. H. MacDonald, Phys. Rev. B **92**, 165121 (2015).
- [49] O. L. Berman and R. Ya. Kezerashvili, Phys. Rev. B **93**, 245410 (2016).
- [50] O. L. Berman and R. Ya. Kezerashvili, Phys. Rev. B **96**, 094502 (2017).
- [51] J. R. Schrieffer, *Theory of Superconductivity* (New York: Benjamin, 1964).
- [52] P. G. De Gennes, *Superconductivity of Metals and Alloys* (W. A. Benjamin, 1966).
- [53] O. L. Berman, R. Ya. Kezerashvili, and K. Ziegler, Physica E **71**, 7 (2015).
- [54] L.D. Landau and E.M. Lifshitz, *Statistical Physics, Part 1* (Pergamon Press; 3rd edition, Oxford, NY, 1980).
- [55] E.M. Lifshitz and L.P. Pitaevskii, *Statistical Physics* (Pergamon Press, Oxford, 1980) Pt. 2.
- [56] H. Lee, K. Paeng and I.S. Kim, Synthetic Metals **244**, 36 (2018).
- [57] E. Surez Morell et al, Phys. Rev. B **82**, 121407 (2010).
- [58] R. Bistritzer and A.H. MacDonald, Proc. Natl. Acad. Sci. USA **108**, 12233 (2011).
- [59] J. M. Ziman, *Principles of the Theory of Solids* (Cambridge University Press; 2nd edition, Cambridge, 1979).
- [60] S. H. Simon, *The Oxford Solid State Basics* (Oxford University Press, Oxford, 2013).

- [61] N. W. Ashcroft and N. D. Mermin, *Solid State Physics* (Sounders College, New York, 1976).
- [62] A. Gonis, *Green functions for ordered and disordered systems* (North-Holland, Amsterdam, 1992).
- [63] K. Tran et al., *Nature* **567**, 71 (2019).
- [64] A. F. Andreev and I. M. Lifshitz, *Sov. Phys. JETP* **29**, 1107 (1969).
- [65] G. V. Chester, *Phys. Rev. A* **2**, 256 (1970).
- [66] M. Boninsegni, A. B. Kuklov, L. Pollet, N. V. Prokof'ev, B. V. Svistunov, and M. Troyer, *Phys. Rev. Lett.* **97**, 080401 (2006).
- [67] A.A. Abrikosov, L.P. Gorkov, and I.E. Dzyaloshinski, *Methods of quantum field theory in statistical physics*, Dover Publications (New York 1975).
- [68] D.Y. Qiu, F.H. da Jornada, and S.G. Louie, *Phys. Rev. Lett.* **111**, 216805 (2013).
- [69] O.L. Berman, R.Ya. Kezerashvili, Yu. E. Lozovik, K. Ziegler, *Physica E* **92**, 1 (2017).